MODELING AND CONTROL OF BALL AND BEAM SYSTEM USING MODEL BASED AND NON-MODEL BASED CONTROL APPROACHES

Mohammad Keshmiri, Ali Fellah Jahromi*, Abolfazl Mohebbi, Mohammad Hadi Amoozgar and Wen-Fang Xie

Department of Mechanical and Industrial Engineering

Concordia University

Montreal, QC, H3G 2W1, Canada

E-mails: m_keshm@encs.concordia.ca, al_fel@encs.concordia.ca*, a_mohebb@encs.concordia.ca, m_amoozg@mie.concordia.ca, wfxie@encs.concordia.ca

Submitted: Dec. 15, 2011 ***Accepted: Jan. 27, 2012*** ***Published: Mar. 1, 2012***

Abstract— The ball and beam system is a laboratory equipment with high nonlinearity in its dynamics. The aims of this research are to model the ball and beam system considering nonlinear factors and coupling effect and to design controllers to control the ball position. The LQR is designed considering two Degrees-of-Freedom and coupling dynamics. The parameters of the LQR are tuned using Genetic Algorithm (GA). Jacobian linearization method is used to linearize the system around operating-point. Due to the noise of the sensor in the experimental setup, a state observer is designed to observe the velocity of the ball. In order to compare the performance of the LQR and study the effect of simplifying assumptions, two control strategies are designed and implemented: Proportional Derivative Integral (PID) as non-model based control strategy, hybrid PID and Linear Quadratic Regulator (LQR) as combination of model based and non-model based control strategies. The experimental results of this research prove the model based control strategies outperforms the non-model based or hybrid controllers in a nonlinear and noisy ball and beam system. In addition, it is shown that the coupling dynamics cannot be eliminated as a simplifying assumption in designing the controller.

Index terms: Ball and beam, proportional derivative integral controller, linear quadratic regulator, genetic algorithm

I. INTRODUCTION

The ball and beam system is one of the most popular and important bench systems for studying control systems. Many classical and modern control methods have been used to stabilize the ball and beam system [1, 2]. The sensor placed on one side of the beam detects the ball role along the beam and its position. An actuator drives the beam to a desired angle, by applying a torque at the end of the beam. Figure 1 shows the ball and beam system (Quanser Model SRV02 and BB01) which is utilized in this research work. The controller regulates the ball position by moving the beam using the motor and overcome the disturbances. The ball and beam system is an inherent unstable system. In other words, the ball position can be changed without limit for a fixed input of beam angle. This property has made the ball and beam system a suitable device to test different control strategies.

Figure 1 Ball and beam system

The ball and beam system has 2 Degrees-of-Freedom (DOFs). The ball is assumed to have friction, rotary moment of inertial and coriolis acceleration during motion on the beam. However, some of the dynamic properties were neglected in the most research work regarding the ball and beam mechanism in order to simplify the dynamic equation of the system [1-7]. *Yu* [1] and *Oh et al.* [3] modeled the ball and beam system, and neglected the coupling effect of the dynamic equations for two DOFs. They controlled the system considering only one DOF to define the motion of the ball on the beam, and suggested two separate control algorithms for motor and ball positions. However, the ball motion and motor angle interact in the real system.

The angular velocity of the beam during the slow motion of the ball has a small value. Therefore, this parameter was neglected in modeling the ball and beam system in [3], [4], [6]. However, when the ball is far from the desired point, the beam should rotate with noticeable

velocity in comparison to the other parameters. In addition, the coriolis acceleration term directly relates to the beam angle. Therefore, in the present research the beam angular velocity is considered in the modeling.

Due to the nonlinearity and complexity of the governing dynamics, some researchers used non-model based control strategies such as Neural Network [7], Fuzzy Logic [3] and PID [4] to control the ball position and beam angle. The non-model based method does not require mathematical procedure to derive dynamic equations and to apply linearization. However, these methods are mainly experience-based and cannot guarantee the stability of the system, which may pose challenge to control the unstable ball and beam system.

The model based control strategies for the ball and beam system can be categorized into two approaches. The first one considers the torque [1] or acceleration [6] of the beam as a control input; and the second one uses the voltage of the motor [4] as input of the system. *Yu* [1] designed a control algorithm assuming that the dynamics of the system consists of two subsystems: the beam and the motor. He neglected the effect of the coupling in the dynamic equations of the beam, motor and beam angular velocity. The author assumed the motor torque as the input of the beam subsystem. *Pang et al.* [6] studied the ball and beam system and designed a Linear Quadratic Regulator (LQR) to control it. They assumed the beam acceleration as the input of the system with two DOFs: ball and beam motions. Based on this assumption they neglected the effect of the motor nonlinearity. However, the real input of the system is the voltage which does not have linear relationship with the beam acceleration or torque.

Rahmat et al. [4] designed a control algorithm using LQR as an optimal control strategy and considering the voltage of the motor as the input of the system. They designed LQR using the linear dynamic equations of model with two DOFs by neglecting the effect of the angular velocity of the beam to linearize the dynamics equations. The results of the research work in simulation showed that the LQR method is an efficient method to control the ball position. However, the sensors in the experimental system are noisy and the beam angular velocity cannot be neglected. *Chang et al.* [8] designed a tracking control strategy for the ball and beam system using a pair of decoupled fuzzy sliding-mode controllers (DFSMCs). The control algorithm is defined based on decoupling dynamic of the system to avoid complexity and nonlinearity due to the coupling dynamic. They considered the coupling effect of the system as scours of disturbance. However, the decoupling dynamic equation may increase the error of the controller. In addition, the fuzzy controller performance strongly depends on the

data margin of the tuning procedure. Therefore, the control gains, which are selected by the fuzzy algorithm, are not reliable for all range of input data.

The present research has focused on three main topics: comparing the performances of model based and non-model based control strategies, studying the coupling effect in the dynamic equations and designing an optimal control strategy considering the system dynamic specifications (i.e. the moment of inertia of the beam and ball, and beam angular velocity). To this end, three control strategies are designed with respect to each of aforementioned topics, and the control algorithms are implemented on a real ball and beam system. The experimental results proved the effect of the coupling dynamic and the beam angular velocity in the modeling of the system. The comparison among three controllers demonstrates that the LQR optimized using GA performs the best.

The rest of the paper organized in seven sections. The modeling of the system and linearization of the system model are presented in section II. Section III explains the control strategies and mathematical procedure of controllers design. The Implementation of the controller, system calibration and state observer design procedure are presented in the section IV. Finally, simulation and experiment results are presented in section V and the concluding remark is given in section VI.

II. MODELING

In order to derive dynamic equations of the ball and beam system, Lagrangian method is used based on the energy balance of the system. The Lagrangian method is utilized to derive the equation of motions for the ball and beam system in the most model based research works on the ball and beam system [1], [9-11].

a. Equations of Motion

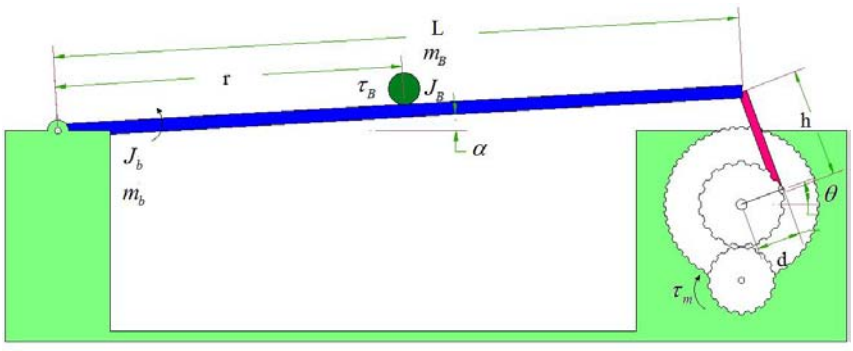

Figure 1 schematic of the ball and beam system

The ball and beam system mechanism of the present study has two DOFs, which is shown in Figure 2, schematically. In order to derive the Euler-Lagrange equation, the first step is to define the kinetic (1) and potential energy (2) for the ball and beam.

$$K = \frac{1}{2} m_B \dot{r}^2 + \frac{1}{2} J_B (\frac{\dot{r}}{R})^2 + \frac{1}{2} (J_B + m_B \dot{r}^2) \dot{\alpha}^2 + \frac{1}{2} J_b \dot{\alpha}^2 \quad (1)$$

$$P = \frac{l}{2} m_b g \sin\alpha + m_B g r \sin\alpha \quad (2)$$

where parameters m_B, m_b, J_b and R are the ball and beam mass, the beam moment of inertia and radius of the ball, respectively; also g and l are the gravity acceleration and length of the beam; variables r and α are the linear motion of the ball along the beam and beam angle.

The difference between kinetic and potential energy is called the Lagrange function, which is defined by L equation (3).

$$L = K_{Kinetic} - P_{Potential} \quad (3)$$

The dynamics equation representing the variation effect of system variable is shown in equation (4). According to equation (4), equation (5) and (6) show the dynamic equation for two DOFs of the ball and beam system.

$$\frac{d}{dt}\left(\frac{\partial L}{\partial \dot{q}}\right) - \frac{\partial L}{\partial q} = Q \quad (4)$$

$$(m_B + \frac{J_B}{R^2})\ddot{r} - m_B \dot{\alpha}^2 r + m_B g \sin c \quad (5)$$

$$(J_B + J_b + m_B r^2)\ddot{\alpha} + 2 m_B r \dot{r} \dot{\alpha} + (\frac{l}{2} m_b + m_B r) g \cos\alpha = \tau \quad (6)$$

where τ is the torque produced by the motor applied on the end of the beam.

b. Linearization around Operating-point of the System

In order to find the linear approximation of the dynamic equations, the Jacobian linearization method is utilized. The output of the Jacobian procedure is the state space equation in the linear format. The mathematical theory of the linearization method should be applied in the state space format. The linear dynamics equation of the ball and beam system can be presented in state space realization [12] as follows.

$$\begin{aligned} \dot{x}(t) &= Ax(t) + BV(t) \\ y(t) &= Cx(t) + DV(t) \end{aligned} \tag{7}$$

$$x_1 = \alpha \quad x_2 = r \quad x_3 = \dot{\alpha} \quad x_4 = \dot{r} \tag{8}$$

where matrix ***A*** defines the dynamic properties of the system; and matrix ***B*** defines the position and properties of the system actuator; matrix ***C*** defines the relation between the states and the output of the system; matrix ***D*** equals zero.

The Jacobian linearization gives the linear dynamic equation around operating point, which is selected to be in the middle of the beam. Consequently, the state space formulation must be derived around operating point. One of the main assumptions used to derive the state-space equation is to define the operation point of the system. It is worth noting that all the states, inputs and outputs with star (*) mark corresponds to the operating point of the system, which are shown as follows:

$$\begin{aligned} \Delta\dot{x} &= A\Delta x + B\Delta u \\ \Delta y &= C\Delta x + D\Delta u \end{aligned} \tag{9}$$

$$\Delta x = \begin{bmatrix} \Delta x_1 \\ \cdot \\ \cdot \\ \Delta x_n \end{bmatrix} = \begin{bmatrix} x_1 - x_1^* \\ \cdot \\ \cdot \\ x_n - x_n^* \end{bmatrix} \tag{10}$$

$$\Delta u = u - u^* \quad \Delta y = y - h(x^*, u^*)$$

$$x_1^* = 0 \quad x_2^* = \delta \quad x_3^* = 0 \quad x_4^* = 0$$

The dynamic equation of the system is expressed in the format of where *f(x)* is given in the equations (11) - (14).

$$f_1 = x_1 \tag{11}$$

$$f_2 = x_4 \tag{12}$$

$$f_3 = \frac{-2m_B x_2 x_3 x_4 - m_B x_2 g - m_b gl + \tau}{J_b + m_B x_2^2} \tag{13}$$

$$f_4 = \frac{5x_3^2 x_2 - 5gx_1}{7} \tag{14}$$

Based on the Jacobian method, matrices ***A*** and ***B*** can be given as equations (15) and (16). The matrices ***C*** and ***D*** do not have nonlinear terms; therefore, the characteristics of the above mentioned matrices do not change. Matrices ***C*** and ***D*** are presented in equations (17) and (18).

$$A = \left[\frac{\partial f_j}{\partial x_i} \right]_{x_1^*, x_2^*, x_3^*, x_4^*, \tau^*} \quad i = 1-4 \quad j = 1-4 \qquad (15)$$

$$B = \left[\frac{\partial f_{1j}(x_2^*, \tau^*)}{\partial \tau} \right] \quad j = 1-4 \qquad (16)$$

$$C = I_{4\times 4} \qquad (17)$$

$$D = 0 \qquad (18)$$

The static load required in the operating point is defined by τ^*:

$$\tau^* = g\left(\frac{m_b l}{2} + m_B r\right) \qquad (19)$$

The laboratory model of the ball and beam system has two sensors to measure the variation of each DOF and a DC motor as the actuator. This actuator is connected to a gearbox with three simple gears and a lever arm. The beam is connected to the other side of the gearbox with the mechanism shown in Figure 1. Consequently, the input of ball and beam control system is voltage. As a result, a relation should be established between the torque and the voltage in ball beam system. Accordingly, the input of the state space model is changed to the voltage the DC motor. The basic equations for the dynamic behavior of the motor are shown in the equations (20) and (21).

$$L_m \dot{I} + R_m I + K_m \dot{\theta}_{motor} = V \qquad (20)$$

$$\tau_{motor} = K_i I \qquad (21)$$

where V and I are the motor voltage and current respectively, θ_{motor} is motor angle, L_m, R_m, K_m and K_i are motor constants, L_m is assumed to be zero.

By substituting equation (20) into equation (21), the formulation to represent the relation of the motor torque and voltage can be shown in equation (22).

$$\tau_{beam} = \frac{K_g K_i \eta_{total}}{R_m} \frac{L}{d} V - \frac{K_g^2 K_i K_m \eta_{total}}{R_m} \frac{L^2}{d^2} \dot{\alpha} \qquad (22)$$

By substituting equation (22) into equation (6), the system input is changed from torque to voltage. Based on the assumption, a voltage V^* should be defined for the operating point, which is shown in the equation (23). The state space equation can be obtained by applying equations (15) and (16) around V^* and the other initial value in the operating point.

$\dot{x} = f(x)$

$$V^* = (\frac{L}{2} m_b g + m_B g \delta) \frac{R_m L}{d K_g K_i \eta_{total}} \tag{23}$$

$$A = \begin{bmatrix} 0 & 0 & 1 & 0 \\ 0 & 0 & 0 & 1 \\ 0 & -\dfrac{m_B J_b g + m_B^2 g \delta_2^2}{\left(J_b + m_B \delta_2^2\right)^2} & -\dfrac{K_g^2 K_i K_m \eta_{total}}{R_m \left(J_b + m_B \delta_2^2\right)} \cdot \dfrac{l^2}{d^2} & 0 \\ -\dfrac{5g}{7} & 0 & 0 & 0 \end{bmatrix} \tag{24}$$

$$B = \begin{bmatrix} 0 & 0 & \dfrac{K_g K_i \eta_{total}}{(J_b + m_B \delta_2^2) R_m} \cdot \dfrac{l}{d} & 0 \end{bmatrix}^T \tag{25}$$

The ball and beam system parameters and DC motor specifications in the present study are shown in Table I.

Table I. Ball and beam system parameters

Symbol	Quantity	Value
g	Gravity acceleration	9.8 (m/s^2)
m_B	Ball mass	0.064 (kg)
m_b	Beam mass	0.65 (kg)
R	Ball radius	0.0254 (m)
l	Beam length	0.425 (m)
d	Lever length	0.12 (m)
δ	Equilibrium point of ball position	0.2 (m)
K_m	Back EMF constant	0.00767 (V.sec/rad)
K_i	Torque constant	0.00767 (N.m)
K_g	Gear ratio	14
R_m	Motor resistance	2.6 (Ω)
η_{motor}	Motor efficiency	0.69
$\eta_{gearbox}$	Gearbox efficiency	0.85

III. CONTROL STRATEGIES

To achieve the best rendering both in the proceedings and from the CD-ROM, we strongly encourage you to use Times-Roman font. In addition, this will give the proceedings a more uniform look. Use a font that is no smaller than nine point type throughout the paper, including figure captions. The purpose of current study is to design a controller based on dynamic model of the ball and beam system and considering coupling dynamic effect between

DOFs. Based on dynamic equations (5) and (6), and state space model equations (24) and (25), a LQR is designed and optimized using GA algorithm. In order to evaluate the performance of suggested control strategy (LQR) and study the coupling dynamic effect and angular velocity of the beam, PID controller and combination of PID controller and LQR (PID-LQR) are designed. The mathematical steps of LQR design and Genetic Algorithm (GA) optimization procedure, PID controller and PID-LQR are presented in following.

a. LQR

LQR controller stabilizes and controls by changing the location of poles of the system to the optimal location. Time response, overshoot and steady state depend on the location of poles. LQR controls the system by a matrix gain given in equation (27). To solve the energy equation (27) of the system, Riccati equation is used, as stated in equation (28), where ***Q*** is a symmetric positive semi-definite matrix and ***R*** is a symmetric positive definite matrix, which have effective role in the required actuating energy. Solving the Riccati equation will result in finding matrix ***S***. The gain of pole placement is obtained from equation (29) by using the ***S*** matrix. Block Diagram of a state space controller is shown in Figure 3 [13].

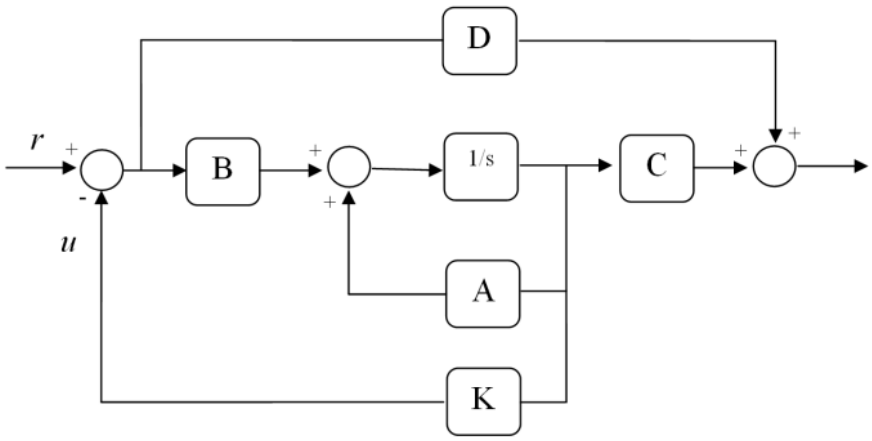

Figure 2. Block diagram of a state feedback controller

$$\dot{x} = (A - KB)x + Br$$
$$y = Cx \tag{26}$$

$$J = \frac{1}{2}\int_0^\infty (x^T(t)Qx(t) + u^T(t)Ru(t))dt \tag{27}$$

$$A^T S + SA - SBR^{-1}B^T S + Q = 0 \tag{28}$$

$$K = R^{-1}B^T S \tag{29}$$

The Ball and Beam system with two DOFs has four poles, two of which are positive, and make the system unstable. Therefore, the main goal of the controller is to move the poles of the system to the left side of S-plane using the gain of the pole placement. The LQR considering coupling dynamic effect is designed based on identified state space equation (24) and (25). Therefore, the LQR is designed based on linearizing around operating point. The input of the system with two DOFs is the DC motor voltage and output is the desired ball position. The matrices *Q* and *R* were selected by trial-and-error in previous section. In order to find the optimal value of the *Q* and *R* matrices regarding the DC motor constraints, GA is utilized for the optimization.

GA is a class of stochastic search optimization methods based on random number generation. The algorithms use only the function values in the search procedure to find a solution. "Genetic algorithms loosely parallel biological evolution and are based on Darwin's theory of natural selection" [14]. The method avoid locally optimum point to find global optimum point based on random search, however the global optimality cannot be proved mathematically [14].

The first step to design GA optimization algorithm is the definition of the objective function to be minimized. The next step is to specify the constrain function to define the feasible region of the actuation system (DC motor). The fitness (objective) function of the GA algorithm is the absolute value of the surround area under the response of ball position for the system with LQR controller. Figure 4 defines the mentioned area, which is utilized for the objective function. This fitness function is introduced in a Matlab code by the numerical integral per iteration. That means the summation of the ball position should be multiplied by the time interval. The fitness function of the optimization procedure is presented in equations (30) and (31).

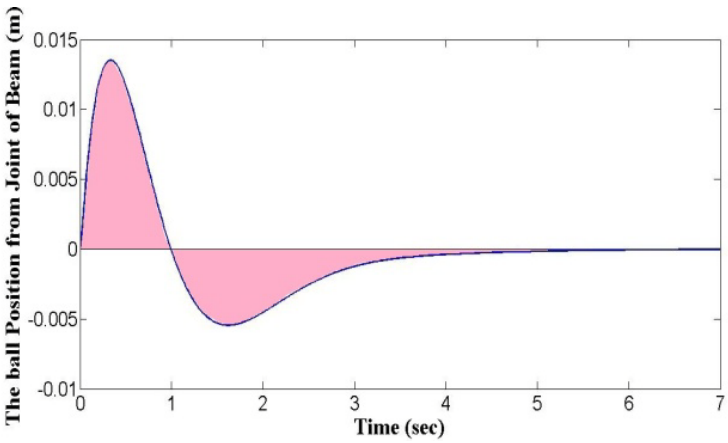

Figure 3 The surrounded area under ball position response of the GA objective function

$$Area = \int_0^t |\dot{x}| dt \qquad (30)$$

$$\dot{x} = (A - KB)x + Br \qquad (31)$$

In order to find the optimal coefficients of matrices ***Q*** and ***R***, the constraint functions should be defined related to the priority of the problem. One of the main constraints is the voltage range for the motor. In other words, the coefficients of matrices ***Q*** and ***R*** should be selected to produce the voltage less than ±8 volt. The other constrains for Genetic Algorithm method is the searching bound for the ***Q*** and ***R***, to make bounded search for satisfying the objective function. In the LQR if the value of the ***Q*** were greater than ***R*** the performance of the controller will increase. As a result, these specifications can be used as a constraint. The constraints of the optimization method are shown in Table II.

Table II Genetic Algorithm Constraint and results

Constrain Function	Lower Bound		Upper Bound	
-8 < *V* < 8	*Q*	*R*	*Q*	*R*
Q>*R*	0.1	0.1	100	10

where V is the input voltage of the DC motor, and it is defined by following equation:

$$V = Kx \qquad (32)$$

The results of GA are presented in Table III. Using the ***Q*** and ***R*** optimized matrices, the LQR gain (33) can be calculated by the presented algorithm.

Table III Results of GA and population size

Population Size	Fitness Function Value	***Q***	***R***
100	0.0067	$72.2*I_4$	0.125

$$K = \begin{bmatrix} 150.98 & -33.18 & 31.94 & -48.63 \end{bmatrix} \qquad (33)$$

b. PID

The PID controller is a well-known industrial feedback control algorithm, which can be designed by both models based and non-model based methods [15]. Figure 5 shows the schematic of this approach for controlling the ball and beam system. Two PID controllers

were designed for the ball position and DC motor, which are described separately in following sections.

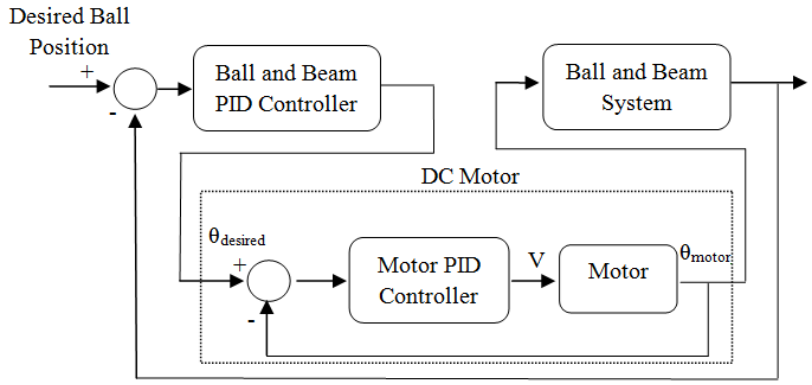

Figure 4 Block diagram of the ball and beam PID control system

The aim of choosing PID as a non-model based control strategy is to study the effect of the dynamic equations in the performance of the control system. In order to study the effect of the coupling in the dynamic equations, the ball and beam system is divided into two subsystems. First, the beam is disconnected from the motor to separately design a PID controller for the motor. The gains are selected based on trail-and-error and Ziegler Nicole method. The PID gains tuned by Ziegler Nicole method [12] are shown in Table IV.

Table IV Ziegler-Nichols motor PID gains

K_p	K_i	K_d
K_{cr} *0.6	P_{cr} *0.5	P_{cr} *0.125
0.12	0.05	0.0125

The ball and beam subsystem, independent to the motor, is an unstable system; therefore, the PID control gains should control and stabilize the system. In order to tune the PID gains the motor control loop should be in series with the ball and beam. The gains can be tuned using trial-and-error. The ball and beam PID gains to control and stabilize system are presented in Table V.

Table V Ball and beam subsystem PID gains

K_p	K_i	K_d
0.7	0.15	0.0375

c. Combination of PID Controller and LQR

One of the solutions for controlling the ball and beam system is to combine different control strategies. Based on the strategy, the nonlinear part is eliminated by neglecting coupling effect of dynamic equations; also, the other controller inside the system covers weak points of the control strategy. The PID-LQR is implemented to study the system without considering the coupling effect in the dynamic equations, which is resulted by dividing the system into two subsystems. The arrangement of the combination of PID controller and LQR is presented in block diagram schematically in Figure 6.

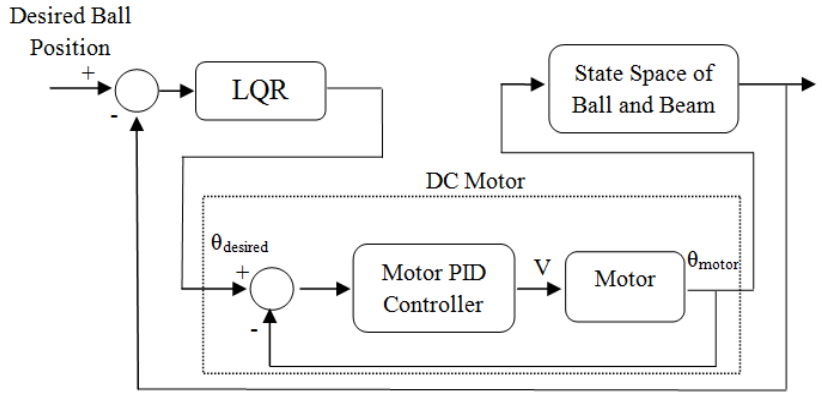

Figure 5 Block diagram of combination of PID control System and LQR

A PID controller is adjusted to control the DC motor. All of the parameters for the PID in this part are the same as the PID controller of the motor presented as before. In order to design the LQR, the dynamic equation of the ball and beam subsystem should be derived. The ball and beam system with considering motor angle (beam rotation) as the input of the system can be modeled as a system with one DOF, which is presented in equation (34).

$$(m_B + \frac{J_B}{R^2})\ddot{r} - m_B\dot{\alpha}^2 r + m_B g \sin(\alpha) = 0 \qquad (34)$$

The beam angle in the section is assumed to be small, therefore sin(α) is approximately equal to α. In addition, the beam angular velocity is of small value, and the square of this parameter is assumed to be neglected. The dynamic equation of the system can be represented in state space format:

$$x = \begin{bmatrix} r & \dot{r} \end{bmatrix}^T \qquad (35)$$

$$\dot{x} = \begin{bmatrix} 0 & 1 \\ 0 & 0 \end{bmatrix} x + \begin{bmatrix} 0 \\ -\frac{5}{7} g \end{bmatrix} \alpha$$
$$y = \begin{bmatrix} 1 & 0 \\ 0 & 1 \end{bmatrix} x \qquad (36)$$

Using the LQR design procedure and identified parameters the LQR gains can be achieved, which are presented as follows:

$$K = \begin{bmatrix} 0.1 & 0.127 \end{bmatrix} \qquad (37)$$

IV. IMPLEMENTATION

In this section, a brief presentation is given on the works that has been done for implementing the controllers on the real system. To control the system, the position of the ball on the beam and the angle of the beam are used as the controller feedback. In order to measure the position of the ball, a sensor is equipped along beam, which is a high resistor metal. A voltage is imposed to the resistor, and the ball connects the resistor to the other rod of the beam (Figure 1). The voltage passed through the second rod is sensed. Depending on the position of the ball the sensed voltage on this rod can be varied from -5 (V) to +5 (V). The effective length of the beam is 42 (cm). If the center of the beam corresponds to zero volt and the sides of the beam correspond to +5 and -5, the position of the ball can be calculated by the following relation.

$$r_b = \frac{2V}{0.42} \qquad (38)$$

where r_b is the position of the ball in centimeters on the beam and V is the voltage sensed by data acquisition. The angle of the beam is calculated as follows:

$$\sin(\alpha) = \frac{d}{l} \sin(\theta) \qquad (39)$$

where θ and α are the angle of the pinion gear (Figure 2) and beam, respectively.

The θ and α variation are small, which can be assumed that sin(θ)≈ θ and sin(α)≈ α. It must be noted that θ is not the angle of motor shaft. Because motor shaft actuation goes through a gear mechanism, and the gear's output is connected to rod h. Consequently, the effect of the gear ratio should be considered into the calculation of the θ angle. Therefore, the relation between θ and α should be presented as follows:

$$\alpha = \frac{d}{lK_g}\theta \qquad (40)$$

A potentiometer is connected to the gear system, which produces a voltage proportional to the motor angle. The voltage range that the potentiometer produce is -5 (V) to +5 (V), and the θ angle range is -180 (deg) to +180 (deg). When θ is -180, the potentiometer gives a voltage of -5 (V), and for +180 (deg) it gives +5 (V). The sensor was calibrated assuming the linear relation between the variation of the voltage and motor angle θ.

The ball and beam system is connected to a desktop computer with a Digital to Analog (D/A) and Analog to Digital (A/D) boards. This board is a PCI board installed on the motherboard of the computer. Programming of the board can be done in Matlab/Simulink. An interface board connects the simulink model to the D/A and A/D boards. The interface board reads the sensor signals, and applies the input voltage to actuate the DC motor.

Reading the sensors and wiring of the system, makes the sensor signals noisy especially for the resistive displacement sensor. The noise causes the problems when the derivative of the data should be calculated numerically from the noisy signals. Using the ball's velocity and the beams angular velocity is inevitable in the system. As a result, a filter or a state observer is required to reduce the noise. A state observer is utilized in the present project, can be adopted for other application independent of specific signal processing toolbox.

The position of the ball and beam angle is measured directly from the sensors, and the derivatives of these positions are obtained through a state observer algorithm. Thus, a reduced observer is used because only two states are needed to be observed [16]. In order to design reduced state observer the known states can be separated from the unknown states as follows:

$$\begin{bmatrix} \dot{X}_m \\ \dot{X}_u \end{bmatrix} = \begin{bmatrix} A_{mm} & A_{mu} \\ A_{um} & A_{uu} \end{bmatrix} \begin{bmatrix} X_m \\ X_u \end{bmatrix} + \begin{bmatrix} B_m \\ B_u \end{bmatrix} V$$
$$y = \begin{bmatrix} I & 0 \end{bmatrix} \begin{bmatrix} X_m \\ X_u \end{bmatrix} \qquad (41)$$

where the index m is related to the known states and index u is related to unknown states.

By rewriting the equation (48), the formulation can be present in format of Eq. (49). The Eq. (49) is the state equation for X_u, and the X_m and V are the system inputs for this equation. The designed state observer of the $\boldsymbol{X_u}$ is present in Eq. (50), which $_{\boldsymbol{u}}$ is the estimated states in the equation .

$$\begin{aligned} \dot{X}_m &= A_{uu}X_u + A_{mu}X_m + B_uV \\ Z &= X_m + A_{mu}X_m - B_mV = A_{mu}X_u \end{aligned} \tag{42}$$

$$\dot{\hat{X}}_m = A_{uu}\hat{X}_u + A_{mu}X_m + B_uV + G(Z - A_{mu}\hat{X}_u) \tag{43}$$

where ***G*** is the observer gain to design reduced state observer, which it presented by the following matrix:

$$G = \begin{bmatrix} 3.6 & 0 \\ 0 & 5 \end{bmatrix} \tag{44}$$

In order to calculate ***Z,*** differentiation of X_m is needed, which it will cause large noises even if X_m have a little noise. By defining Eq. (53) and (54), the ψ can be calculated; following that, by integrating Eq. (54), $_u$ can be achieved from equation (53). Figure 7 shows the comparison between the observed ball velocity and actual signal of the system calculated using numerical derivative, to present the performance of state observer.

$$\dot{\hat{X}}_m = \psi + GX_m \tag{45}$$

$$\begin{aligned} \dot{\psi} &= (A_{uu} - GX_{mu})\psi \\ &+(A_{uu}G + A_{um} - GA_{mm} - GA_{mu}G)X_m \\ &+(B_u - GB_m)V \end{aligned} \tag{46}$$

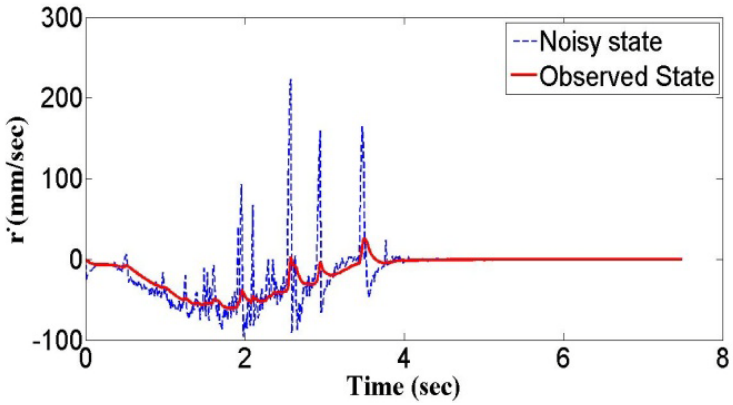

Figure 6 Measured and Observed Signal

During implementation, as the system was set to run, a relatively large difference exists between the actual and desired position of the ball. The system aims to reduce this error;

therefore, a big actuation input is imposed to the actuator. The actuation of the motor makes the sudden motion in the beam, which it may cause the ball to jump, and lose its contact from the beam. Losing the contact leads to loss of the position signal; as a result, it will leads to the system failure. In order to prevent these abrupt movements, the desired point should not be a sharp step. Instead, system needs a smooth path that starts from the actual ball position, and ends at the desired position. To create such path, a first order system is located right after the step function. The following first order system is used in implementations.

$$f = \frac{20}{s+20} \qquad (47)$$

V. RESULT AND DISCUSSION

The PID control strategy was designed non-model based. Thus, the gains of two PID controllers should be designed in closed loop system in an experimental set. In addition, since the combination of PID-LQR is designed based on a non-model based method it can only be evaluated on the experiment setup. However, the gain of the LQR was tuned based on mathematical solution as explained previously. In order to evaluate and compare the result of the PID and PID-LQR, the experimental results for the ball position and motor beam angle responses are shown in Figures 8 and 9.

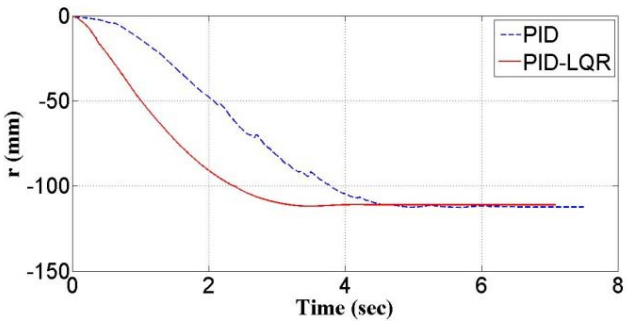

Figure 7 The ball position response using the PID controller and PID-LQR

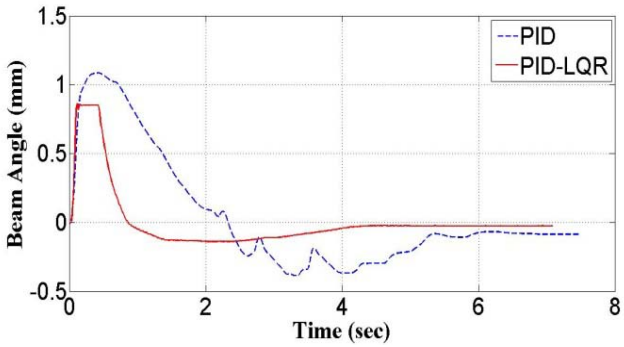

Figure 8 The beam angel response using the PID controller and PID-LQR

Figs. 8 and 9 show the PID-LQR are more efficient than non-model based PID controller, also show both controllers make the system stable. The desired point for both experiments is 10 cm far from the right hand side of the beam's middle point. Based on the desired ball position, the diagrams show both control strategies have steady state error. The steady state error, settling time (5% criteria [11]) and overshot of the PID-LQR are lower than those of PID controller. Based on the experimental results of the ball and beam system, the model based controller are more efficient than non-model based.

The main challenge of this research work is to design LQR considering effect of coupling dynamic and system specification (i.e. the beam angular velocity and coriolis acceleration). The LQR is designed based on two DOFs, therefore the controller can be simulated and tuned before implementation. The simulation and experimental results of LQR optimized using GA are shown in Figs. 10 and 11 to evaluate the accuracy of the model used to deign LQR.

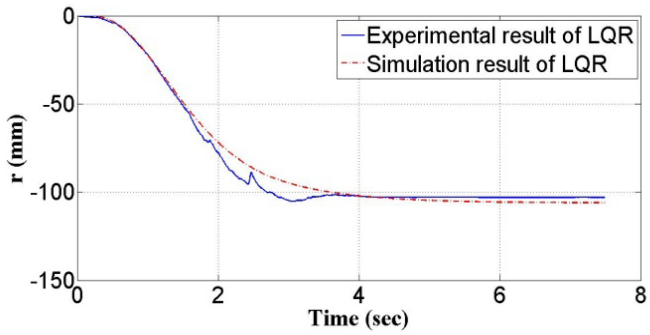

Figure 9 The ball position response using the LQR in the simulation and experiment

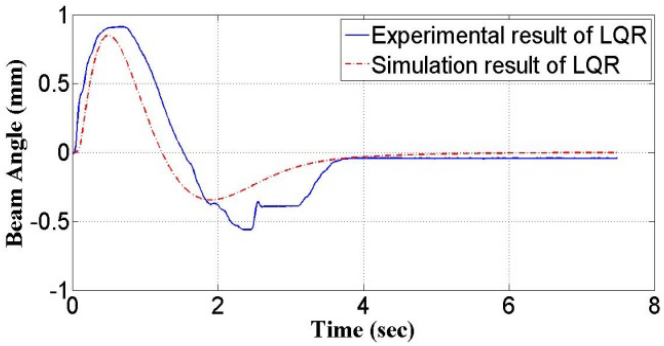

Figure 10 The beam angle response using the LQR in the simulation and experiment

Figs. 10 and 11 present the defined model for the ball and beam system. Based on the derived dynamic model, the response of the system can be simulated with high accuracy (considering the noise effect). In order to compare the performance of the optimized LQR with two DOFs using GA with non-optimized LQR and non-model based PID, the experimental results for

PID controller, PID-LQR and LQR are presented for the same experiment in Figures 12 and 13.

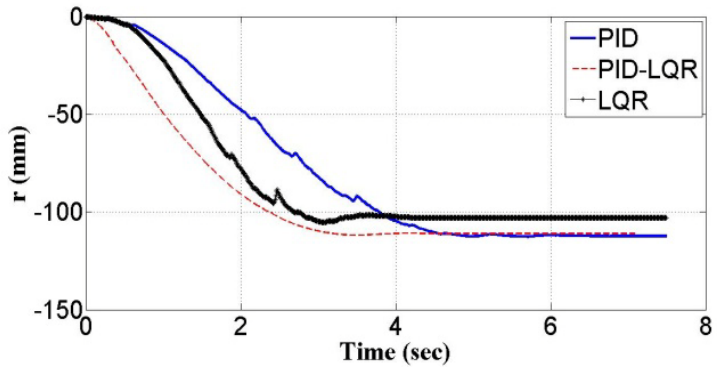

Figure 11 The ball position response using the PID controller, PID-LQR and optimized LQR using GA

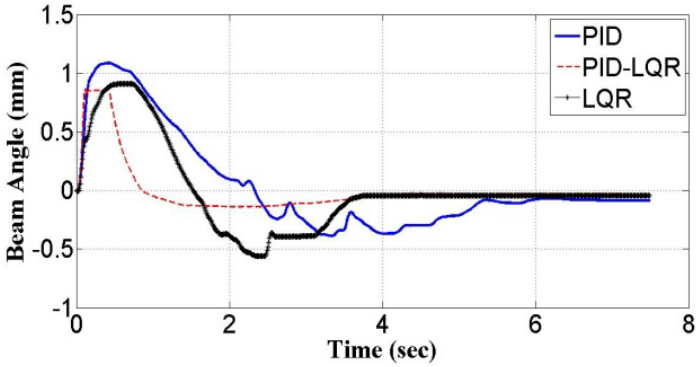

Figure 12 The beam angle response using the PID controller, PID-LQR and optimized LQR using GA

The optimized LQR using GA shown in Figs. 12 and 13, have the lowest steady state error. The Figs. 12 and 13 show that the LQR, as an optimal model based control strategy, are more efficient than non-model based. In addition, these figures show the coupling dynamic effect and angular velocity of the beam are not neglectable. The controller performances of three control strategies are shown in Table VI.

Table VI The ball position response specification

Controller	Settling Time (5%)	Steady State Error
PID	6.053 (sec)	11.9%
PID-LQR	3.958 (sec)	11%
LQR	4.156 (sec)	2.9%

In order to evaluate the effect of GA, the required voltages for three controller strategies are shown in Figure 14 to compare the required actuating energy and voltage in controlling the ball and beam system. The figure shows that the LQR actuation commands to DC motor are within the defined voltage range in GA. Furthermore, the required voltage for optimized LQR is lower than PID and PID-LQR. Comparing the settling times, one can see that with less energy consumptions the settling time for LQR is approximately the same as that for LQR-PID method. It can be also seen that the required voltage for the PID-LQR ($-15.8<V<8.4$) is outside of the critical working region of the DC motor, which may damage the motor.

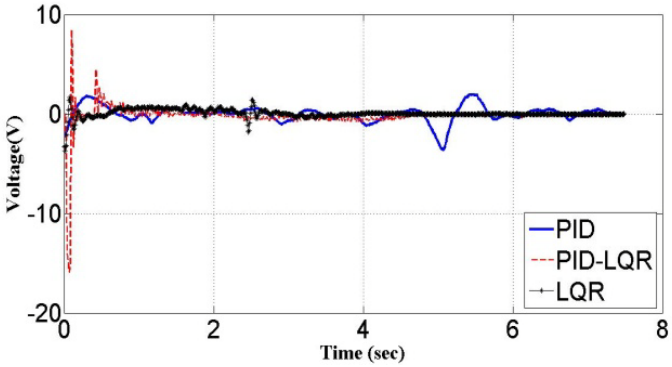

Figure 13 The required voltage for the actuation of the DC motor using the PID controller, PID-LQR and optimized LQR using GA

VI. CONCLUSION

The current research work is devoted to study three different control strategies for the ball and beam system including PID controller, PID-LQR and LQR with different assumptions in the dynamic modeling and tuning method. The PID controller is designed without using dynamic equations as a non-model based method. The PID-LQR is design as combination of simplified model based and non-model based method neglecting the coupling effect dynamic equation and angular velocity of the beam. The LQR is designed considering the coupling effects and the nonlinearity of the model. The weight matrices $\boldsymbol{Q}$ and $\boldsymbol{R}$ are optimized using GA. The implementation technique of the controllers in the experimental setup is explained, and a reduced state observer is designed to predict the noisy state based on the dynamic of the system. The experimental results proved the effect of the coupling dynamic and the beam angular velocity in the modeling of the system, and efficiency of the optimized LQR using GA. In addition, the voltage diagram of the motor for different controllers presents that the effect of the GA as an optimization algorithm to minimize actuation energy of the system.

VII. ACKNOWLEDGMENT

We would like to thanks Dr. Chun-Yi Su for his invaluable comments in the conceptualization of the project. In addition, the authors would like to thanks Concordia University mechatronics laboratory staff for their assist and support to our group in fulfilling the project.

REFERENCES

[1] W. Yu, "Nonlinear PD Regulation for Ball and Beam System", International Journal of Electrical Engineering Education, Vol. 46, pp. 37–59, 2009.

[2] Li X. and Yu W., "Synchronization of Ball and Beam Systems with Neural Compensation", International Journal of Control, Automation and Systems, Vol. 8, No. 3, pp.491-496, 2010.

[3] S.K Oh, H.J. Jang and W. Pedrycz, "The Design of a Fuzzy Cascade Controller for Ball and Beam System: A Study in Optimization with the Use of Parallel Genetic Algorithms", Engineering Applications of Artificial Intelligence, Vol. 22, pp. 261–271, 2009.

[4] M.F. Rahmat, H. Wahid and N.A. Wahab, "Application of Intelligent Controller in a Ball and Beam Control System", International Journal on Smart Sensing and Intelligent Systems, Vol. 3, pp. 45–60, 2000.

[5] P.T. Chan, W.F. Xie and A.B. Rad, "Tuning of Fuzzy Controller for an Open-loop Unstable System: a Genetic Approach", Fuzzy Sets and Systems, Vol. 111, pp. 137–152, 2000.

[6] Z.H Pang, G. Zheng and C.X. Luo, "Augmented State Estimation and LQR Control for a Ball and Beam System", Proc. of the 6th IEEE Conference on Industrial Electronics and Applications (ICIEA), pp.1328-1332, June 21-23, 2011.

[7] H. Verrelst, K. Van Acker, J. Suykens, B. Motmans, B. De Moor and J. Vandewalle, "NLq Neural Control Theory: Case Study for a Ball and Beam System", Proc. of the European Control Conference (ECC'97), Brussels, Belgium, July 1–4, 1997.

[8] Y.H. Chang, C.W. Chang, C.W. Tao, H.W. Lin and J.S. Taur, "Fuzzy Sliding-mode Control for Ball and Beam System with Fuzzy ant Colony Optimization", Expert Systems with Applications, Vol. 39, No. 3, pp. 3624-3633, 2012.

[9] F.O. Rodriguez, W. Yu, R.L. Feregrino and J.J.M. Serrano, "Stable PD Control for Ball and Beam System", Proc. of the International Symposium on Robotics and Automation 2004, Quereturo, Mexico, August 24-27, 2004.

[10] W. Yu and F. Ortiz, “Stability Analysis of PD Regulation for Ball and Beam System”, Proc. of the IEEE Conference on Control Applications, Toronto, Canada, August 28-31, 2005.

[11] D. Colon and I.S. Diniz, “Teaching and Comparing Advanced Control Techniques in a Ball and Beam Didactical Plant”, Proc. of the 20th International Congress of Mechanical Engineering, Gramado, RS, Brazil, November 15-20, 2009.

[12] K. Ogata. Modern Control Engineering. 3rd ed., New Jersey: Prentice Hall, 1997.

[13] A.F. Jahromi; and A. Zabihollah, “Linear Quadratic Regulator and Fuzzy Controller Application in Full-car Model of Suspension System with Magnetorheological Shock Absorber”, Proc. of the IEEE/ASME International Conference on Mechatronics and Embedded Systems and Applications (MESA), pp. 522–528, July 15–17, 2010.

[14] J. S. Arora, Introduction to Optimum Design. 2ed ed., California, USA: Elsevier Academic Press, 2004.

[15] Fox, Charles. An Introduction to the Calculus of Variations. New York, USA: Courier Dover Publications, 1987.

[16] Pierre R. Bélanger, Control Engineering: A Modern Approach, USA: Saunders College Pub., 1995.